USAFSAM-TP-90-24

PROTON ARC DOSES TO THE PRIMATE HEAD

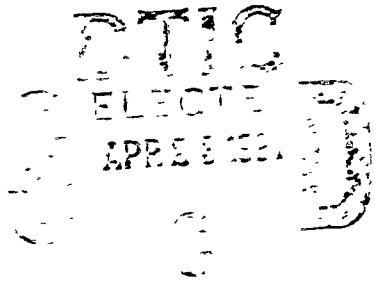

Dennis D. Leavitt, Ph.D.

Texas A&M Research Foundation , Inc.
Box 3578
College Station, TX 77843

December 1990

Final Report for Period November 1989 - September 1990

Prepared for
USAF SCHOOL OF AEROSPACE MEDICINE
Human Systems Division (AFSC)
Brooks Air Force Base, TX 78235-5301

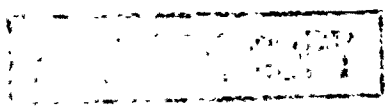

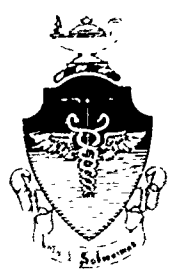

NOTICES

This final report was submitted by Texas A&M Research Foundation, Inc., Box 3578, College Station, Texas, under contract F33615-87-D-0627/0009, job order 7757-04-41, with the USAF School of Aerospace Medicine, Human Systems Division, AFSC, Brooks Air Force Base, Texas. Mr. Kenneth A. Hardy (USAFSAM/RZB) was the Laboratory Project Scientist-in-Charge.

When Government drawings, specifications, or other data are used for any purpose other than in connection with a definitely Government-related procurement, the United States Government incurs no responsibility or any obligation whatsoever. The fact that the Government may have formulated or in any way supplied the said drawings, specifications, or other data, is not to be regarded by implication, or otherwise in any manner construed, as licensing the holder or any other person or corporation; or as conveying any rights or permission to manufacture, use, or sell any patented invention that may in any way be related thereto.

The animals involved in this study were procured, maintained, and used in accordance with the Animal Welfare Act and the "Guide for the Care and Use of Laboratory Animals" prepared by the Institute of Laboratory Animal Resources - National Research Council.

The Office of Public Affairs has reviewed this report, and it is releasable to the National Technical Information Service, where it will be available to the general public including foreign nationals.

This report has been reviewed and is approved for publication.

Kenneth A. Hardy

KENNETH A. HARDY, M.S.
Project Scientist

STANLEY L. HARTGRAVES, Lt Col, USAF, BSC
Supervisor

George Schwender MD

GEORGE E. SCHWENDER, Colonel, USAF, MC, CFS
Commander

REPORT DOCUMENTATION PAGE

Form Approved
OMB No. 0704-0188

1a. REPORT SECURITY CLASSIFICATION Unclassified	1b. RESTRICTIVE MARKINGS
2a. SECURITY CLASSIFICATION AUTHORITY	3. DISTRIBUTION/AVAILABILITY OF REPORT Approved for public release; distribution is unlimited.
2b. DECLASSIFICATION/DOWNGRADING SCHEDULE	
4. PERFORMING ORGANIZATION REPORT NUMBER(S)	5. MONITORING ORGANIZATION REPORT NUMBER(S) USAFSAM-TP-90-24
6a. NAME OF PERFORMING ORGANIZATION Texas A&M Research Foundation, Inc. 6b. OFFICE SYMBOL (If applicable)	7a. NAME OF MONITORING ORGANIZATION USAF School of Aerospace Medicine (RZB)
6c. ADDRESS (City, State, and ZIP Code) Box 3578 College Station, TX 77843	7b. ADDRESS (City, State, and ZIP Code) Human Systems Division (AFSC) Brooks AFB TX 78235-5301
8a. NAME OF FUNDING/SPONSORING ORGANIZATION 8b. OFFICE SYMBOL (If applicable)	9. PROCUREMENT INSTRUMENT IDENTIFICATION NUMBER F33615-87-D-0627/0009
8c. ADDRESS (City, State, and ZIP Code)	10. SOURCE OF FUNDING NUMBERS

PROGRAM ELEMENT NO.	PROJECT NO.	TASK NO.	WORK UNIT ACCESSION NO.
62202F	7757	04	41

11. TITLE (Include Security Classification)
Proton Arc Doses to the Primate Head

12. PERSONAL AUTHOR(S)
Leavitt, Dennis D.

13a. TYPE OF REPORT	13b. TIME COVERED	14. DATE OF REPORT (Year, Month, Day)	15. PAGE COUNT
Final	FROM 89/11/30 TO 90/09/30	1990, December	22

16. SUPPLEMENTARY NOTATION
Research protocol RZB 82-01.

17. COSATI CODES		
FIELD	GROUP	SUB-GROUP
06	07	
03	02	

18. SUBJECT TERMS (Continue on reverse if necessary and identify by block number)
Depth dose distribution; Solar flare protons; Radiation dosimetry; Space radiation.

19. ABSTRACT (Continue on reverse if necessary and identify by block number)

The radiation dose distributions to the primate head are calculated for 10 MeV, 32 MeV, 55 MeV, and 110 MeV protons incident on the primate. Rotation of the primate in the field is simulated by summing a 360-degree arc in 1/2 degree increments. Representative anatomy is determined by Computerized Tomography scans of a primate head phantom. Dose-volume histograms are used to compare the dose to the brain for each of the four irradiation techniques. Surface dose and depth dose calculations are made to evaluate the dosimetric effects to the primate eye. Estimates are made of the effects of irradiation with the primate eyes open versus closed. A focusing effect is described to explain the localized high doses seen with 32 MeV and 55 MeV proton exposures. Doses to the eye are calculated and tabulated by animal identification key for a series of irradiated primates. These calculations demonstrate significant departures from the dose predictions based on simple cylindrical phantoms, suggesting that careful review of the primate dosimetry must accompany any evaluation of radiation effects on these animals.

20. DISTRIBUTION/AVAILABILITY OF ABSTRACT	21. ABSTRACT SECURITY CLASSIFICATION	
☒ UNCLASSIFIED/UNLIMITED ☐ SAME AS RPT. ☐ DTIC USERS	Unclassified	
22a NAME OF RESPONSIBLE INDIVIDUAL Kenneth A. Hardy	22b. TELEPHONE (Include Area Code) (512) 536-3417	22c. OFFICE SYMBOL USAFSAM/RZB

DD Form 1473, JUN 86 *Previous editions are obsolete.*

PROTON ARC DOSES TO THE PRIMATE HEAD

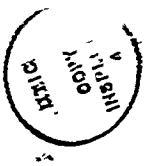

INTRODUCTION

Since the initial irradiation of primates with proton energies from 32 to 400 MeV in 1966 (1), continued interest in the radiation effects exhibited by these primates has led to retrospective evaluation of the probable dose distributions within the primate head (2). Additionally, the prospective solar flare radiation dose distribution within the head of a standard man phantom has been evaluated using computerized radiation therapy treatment planning programs (3). These reports suggested that, for the 55-MeV proton irradiation, portions of the primate brain may have received doses as high as three times the surface dose by which the exposures were calibrated. They also suggested that for the three solar flare irradiations studied, substantial doses could be delivered to vital areas of the brain relative to the surface, particularly in the glial cell region. Continuing radiobiological evaluation of the irradiated primates has found variable radiation effects to the eye, wherein primates irradiated to the same apparent dose exhibit differing radiation response. This report compares the dose distribution to the primate head for four proton energies which are representative of experimentally used beams and evaluates the calculated surface dose, dose distribution through the eye, and doses to the primate brain. Doses to the brain are compared by dose-volume histogram techniques. Additionally, doses received by individual labeled primates are calculated based on the tabulated surface dose assigned to those primates at the time of initial irradiation.

METHODS AND MATERIALS

Four proton energies were used to calculate the dose distribution to the primate head, with particular emphasis on dose to the eye, resulting from irradiation in a proton field while rotating about the principal axis of

the primate. The static field depth doses for the four proton energies of 10, 32, 55 and 110 MeV, as determined from published and unpublished reports (1,4), are shown in Figure 1. This figure illustrates the difference in range of the proton beams, from 1 cm for 32 MeV to nearly 10.5 cm for 110 MeV. Additionally, this figure demonstrates the increased dose due to the Bragg peak for the 32, 55 and 110 MeV protons. This figure shows a maximum dose, relative to the surface dose, of 11 for 32 MeV, 6.3 for 55 MeV, and 2.4 for 110 MeV. No Bragg peak is shown for the 10 MeV beam, as this was a beam which was degraded from a higher energy beam.

Doses were calculated as in the earlier reports. A radiation therapy treatment planning program in clinical use was applied to calculate the dose distributions due to protons incident on the primate head. This treatment planning program calculates the radiation dose as the product of a central axis depth dose (corrected for inverse square law dependence and for density of structures intersecting the ray) and an off-axis factor representing the change in field intensity away from the central axis. For this study the central axis depth doses were entered from a table of data used in the original measurements; the off-axis factors were set to one, since the isoflux profiles suggested that this approximation was valid for at least the central 10 cm of the field in both lateral and vertical directions (1). The relative biological effect (RBE) of the proton field was considered to be constant across the range of the protons (5).

Previously determined computerized tomography (CT) scans of a primate head phantom extending in parallel slices spaced 0.5 cm apart from the base of the skull to the top of the head were used. The internal anatomy of the phantom was determined from these CT slices. A "patient contour" corresponding to each of these CT slices was entered into the treatment planning computer. The external patient contour was determined by automatic contour tracing of the air-phantom interface. The internal contours representing the skull were likewise determined by automatic contour tracing, and an average density was determined for each structure by examining all the CT density values corresponding to CT pixels within that internal contour. Thus, variation in the density of bone throughout the skull is accounted for slice-by-slice and an average density

is attached to each structure within each slice. A target volume within which dose-volume histogram analysis would be performed was determined by manually tracing the area representing the brain within each CT slice. Eleven planes, representing a cranio-caudad distance of 5 cm from the most inferior to most superior, were entered from CT data. Additional contours were added by interpolation between CT slices for a total of 20 calculation planes separated by 0.25 cm. Reference points were entered in 1-mm increments along a line bisecting the eye. These reference points were used to evaluate the depth doses through the eye.

Dose distributions were calculated by treating the rotation of the primate head in the proton beam as the summation of doses for fields directed toward an isocenter in the approximate center of the primate head, equally weighted, and spaced in 0.5 degree angular increments through a full 360 degrees. This calculation is similar to the numerical integration techniques reported in the original paper; however, this calculation takes into account the departure from cylindrical shape of the primate phantom, as well as the additional dose attenuation introduced by the higher density skull. These calculations were repeated for each of the 20 planes. In each plane a calculation and display grid of 9,200 points yielded a grid spacing of 0.8 mm. From this grid isodose curves were plotted which demonstrate the variation in dose in two-dimensional space across each calculational plane of the phantom. A volume histogram of all calculation points within the brain volume was calculated.

RESULTS

The relative surface dose, normalized to a 10-cm diameter cylinder, was calculated for each of the incident proton energies for cylinders from 5-cm to 15-cm diameter and are shown in Figure 2. These calculations were based on numerical integration of the depth doses shown in Figure 1 in 0.1-degree increments through a full 360 degrees of arc (6). Due to the range of the protons, a point on the surface of the cylinder is irradiated by the proton beam for greater than 180 degrees of arc, thereby increasing the surface dose as the cylinder diameter decreases. In the case of the

110-MeV proton exposure, the 10.5-cm proton range means that a point on the surface of any cylinder of diameter less than 10.5 cm will be irradiated during the entire 360 degrees of arc. The increased dose in the range of the Bragg peak produces a maximum surface dose for a cylinder of approximately 8.5 cm diameter. For cylinders of lesser diameter, the Bragg peak is beyond the distal surface of the cylinder, and therefore the surface dose is reduced. Since the diameter of the primate head at the level of the eyes is approximately 8 cm, an increased surface dose to the eyes can be expected, relative to the dose normalization based on a 10-cm diameter cylinder. For the 110-MeV component, this increase may be as much as 17% while for the 10-MeV component the dose increase may be only 2%.

Earlier work demonstrated that the shape of the primate head can introduce large changes in dose distribution, relative to the cylindrical shape. To evaluate this effect, depth doses through the primate eye were calculated and compared with depth dose calculations based on a cylinder diameter of 8 cm. For the 10-MeV protons, calculations indicated approximately 105% of surface dose relative to a 10-cm diameter cylinder, compared to 102% for the 8-cm cylinder calculation. A greater dose at all depths is also seen, as illustrated in Figure 3A. The greater dose is attributed to the small radius of curvature of the eye, compared to the rest of the head, thereby allowing increased penetration of the protons into the eye through a segment of the arc, compared to that through a standard cylinder. This effect is more pronounced for 32 MeV protons, illustrated in Figure 3B. Here the surface dose increases to 124%, compared to 102.5% for the 8-cm diameter cylinder. However, since the Bragg peak for 32-MeV protons occurs at slightly less than 1-cm depth, a very dramatic enhancement of dose within the eye is seen at a depth of about 0.85 cm, as this depth serves as a focus for the Bragg peak as the primate eye rotates through the beam. This dose enhancement is calculated to be 311% of surface dose to a 10-cm diameter cylinder. For comparison, the maximum dose calculated within an 8-cm diameter cylinder is 135% of surface dose to a 10-cm diameter cylinder. This focusing effect of the Bragg peak within the primate eye produces a very high dose to a very small volume. This effect is illustrated in the isodose curves in Figure 4 calculated for

each proton energy. Similar results are seen in Figure 3C for the 55-MeV proton dose calculations. Here the surface dose to the eye is calculated to be 116%, compared to 106% for an 8-cm diameter cylinder. An increased dose of 168% is seen at a depth of 1.85 cm compared to a dose of 139% at the same depth in an 8-cm diameter cylinder, suggesting some focusing of the Bragg peak at this depth in the eye. Further dose enhancement is seen at depths greater than the dimension of the eye, from 2.0- to 2.6-cm depth. This change may be significant in that this high dose of up to 193% may be received by the optic nerve extending beyond the eye. Finally, Figure 3D illustrates the depth doses to the primate eye and to the 8-cm diameter cylinder for 110-MeV protons. The surface dose to the eye is seen to be approximately 115% of surface dose to the 10-cm cylinder, rising to 120% within 1 mm of the surface and remaining uniform across the dimension of the eye. Similarly, the dose within the 8-cm cylinder remains at about 115% across the dimension of the cylinder.

To evaluate the possible change in dose distribution due to irradiation of the primate with its eyes closed, rather than open, the external contour corresponding to the eye was modified and the dose calculations repeated. One millimeter thickness was added to the contour surrounding the eye, corresponding to the estimated thickness of the primate eyelid. The reference points were left in their same locations, and the arc calculations were repeated using the same beam weighting and calculation increments. The differences seen were as follows: (a) for 10-MeV protons the dose to the surface of the eye was reduced by 2%, corresponding to the attenuation through the additional thickness of eyelid tissue, and the depth dose through the eye was commensurately reduced; (b) for 32-MeV protons the dose to the surface of the eye increased to 140% and the maximum dose increased to 377% at a depth of 8 mm behind the front surface of the eye; (c) for 55-MeV protons the dose on the surface of the eye increased by 2.5%, reflecting the dose buildup through the eyelid, while the depth doses through the eye increased by 1 to 2%; and (d) for 110-MeV protons an increase of less that 1% was noted. Thus, the greatest effect was seen with the 32-MeV proton irradiation. The effect of irradiation with eyelids closed vs. open could change the dose to the surface of the eye by as much as 10%, while moving the depth of the

peak dose by the thickness of the overlying eyelid. This change may, in part, account for the variability in results observed in radiation effects to the eyes of primates irradiated using 32-MeV protons.

Using the primate head outline, depth doses were calculated corresponding to exposures of 10-MeV and 110-MeV protons received by the primates. These doses are listed in Table 1 according to primate identification, and are tabulated to a depth of 1.8 cm, corresponding to the boundary of the eye and the skull. Three different irradiation schemes were effected in the original exposures: 10-MeV protons plus 110-MeV protons; 10-MeV protons only; and 110-MeV protons only. For the 10-MeV and combined 10-MeV and 110-MeV exposures, the exposures were graduated to deliver an estimated surface dose from 300 CGy to 1,800 CGy in steps of 300 CGy. The present calculations indicate that the surface dose delivered by the 10-MeV beam only closely matches the surface dose resulting from the combined 10-MeV plus 110-MeV exposures for each dose increment. However, the 10-MeV depth dose decreases more rapidly than the combined depth dose, and actually delivers a lower dose to the back of the eye than either the combined irradiation or the 110-MeV component alone. Depth doses for four irradiation schemes are plotted in Figure 5.

The differences in dose distribution to the primate brain due to irradiation from 10-, 32-, 55-, or 110-MeV protons were studied by dose volume histogram. Using a field weighting which would deliver 100% dose to the surface of a 10-cm diameter cylinder for each proton energy, the dose distributions were calculated in 20 equally spaced parallel planes across the primate head, and the pixel points within the brain contour for each plane were sorted and summed by dose value. The comparative dose volume histograms are shown in Figure 6. These histograms demonstrate that no significant dose to the brain is received from either the 10-MeV or the 32-MeV proton irradiation. Over 50% of the brain volume irradiated with 55-MeV protons received a dose from 100% to 150% of the reference surface dose, while 20% of the brain volume received a dose of 5% or less. The maximum dose received anywhere within the brain volume was 382%. Calculation of 110-MeV proton irradiation showed 96% of the brain volume

receiving a dose between 105% and 125% of the reference surface dose. Representative isodose distributions are shown in Figure 4 for each proton beam energy.

CONCLUSIONS

For all energies studied, the calculated surface dose to the primate head was higher than that predicted from calculation using a simple cylinder approximation. The surface dose ranged from 105% to 124% of surface dose for a 10-cm diameter cylinder.

The focusing effect was most pronounced for 32-MeV and 55-MeV protons. This effect introduced a dose increase of up to 311% for 32 MeV and 193% for 55 MeV in the plane of the eye.

The distribution of dose to the brain is strongly dependent on the energy of the proton beam used. The range of the 10-MeV and 32-MeV beams is inadequate to deliver significant dose to the brain; however, the range of the 55-MeV protons is adequate to place the Bragg peak of the proton distribution fully within the brain during most of the arc, thereby producing areas of high dose within the brain relative to the surface dose. The range of the 110-MeV protons enables the entire brain to be irradiated during the complete arc, leading to a reasonably uniform dose distribution throughout the brain.

Each of these departures from the dose predictions of a simple cylinder may have significance in the continuing evaluation of radiation dose effects, as an accurate estimate of delivered dose is necessary to validate interpretation of radiation response.

REFERENCES

1. Williams, G.H., Hall, J.D., and Morgan, I.L. Whole-body irradiation of primates with protons of energies to 400 MeV. ***Radiat Res*** **28**:372-389 (1966).

2. Leavitt, D.D. Analysis of Primate Head Irradiation with 55 MeV Protons. ***Radiat Res*** (In Press, 1990).

3. Leavitt, D.D. Proton Depth Dose Distribution: 3-D Calculation of Dose Distributions from Solar Flare Irradiation. USAFSAM-TP-90-17, November 1990.

4. Burton, B.S., Parker, C.V., Boles, L.A., Alexander, E.F., and Nelson, J.B. Simulation and Measurement of Solar-Flare Proton Exposures. SAM-TR-70-38, June 1970, Accession Number AD-711-041.

5. Goitein, M., Urie, M., Munzenrider, J.E., Gentry, R., Lyman, J.T., Chen, G.T.Y., Castro, J.R., Maor, M.H., Stafford, P.M., Sontag, M.R., Altschuler, M.D., Block, P., Chu, J.C.H., and Richter, M.P. Report of the working groups on the evaluation of treatment planning for particle beam radiotherapy. p.5.5.1. Published by the Radiotherapy Development Branch, Radiation Research Program, Division of Cancer Treatment, National Cancer Institute, Sandra Zink, Project Officer.

6. Mitchell, J.C., Dalrymple, G.V., Williams, G.H., Hall, J.D., and Morgan, I. Proton Depth-Dose Dosimetry. ***Radiat Res*** **28**:390-405 (1966).

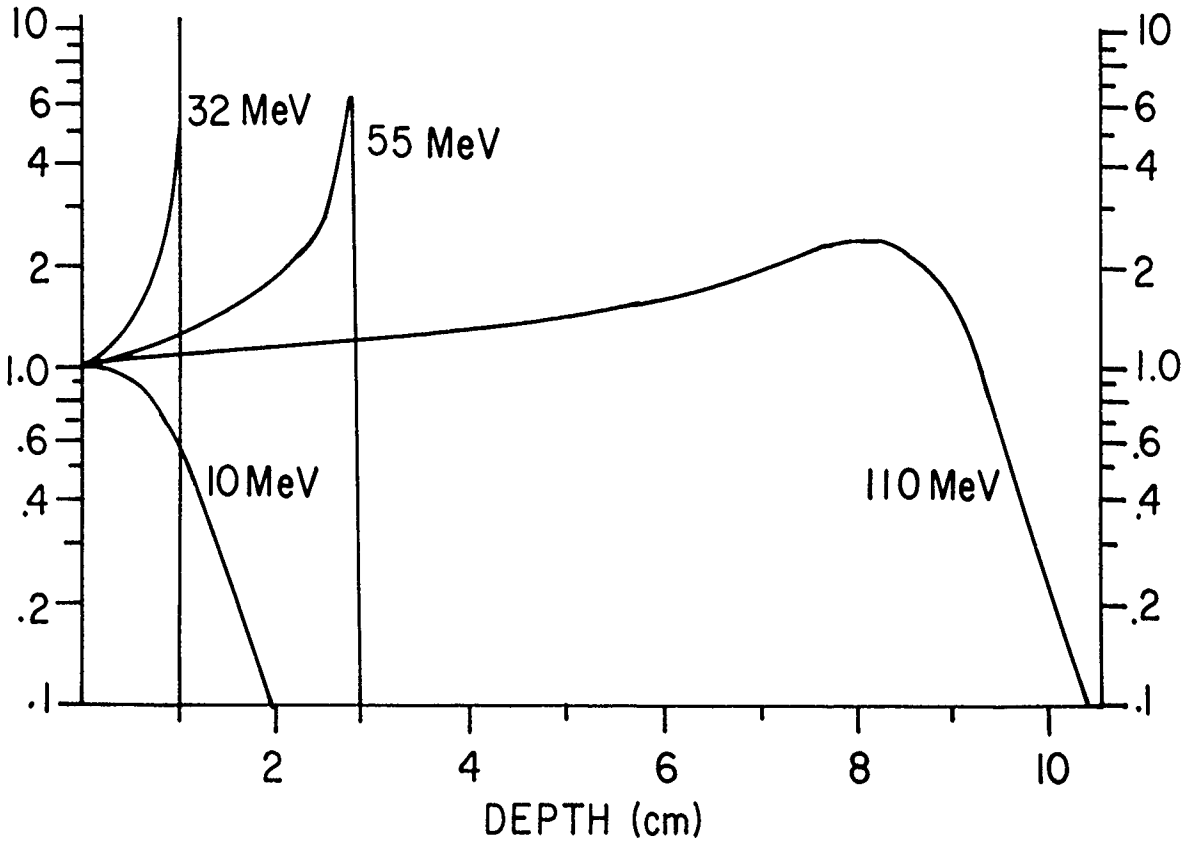

Figure 1. Static field proton depth doses for 10-MeV, 32-MeV, 55-MeV and 110-MeV protons. Each curve is normalized to 1.0 on the phantom surface.

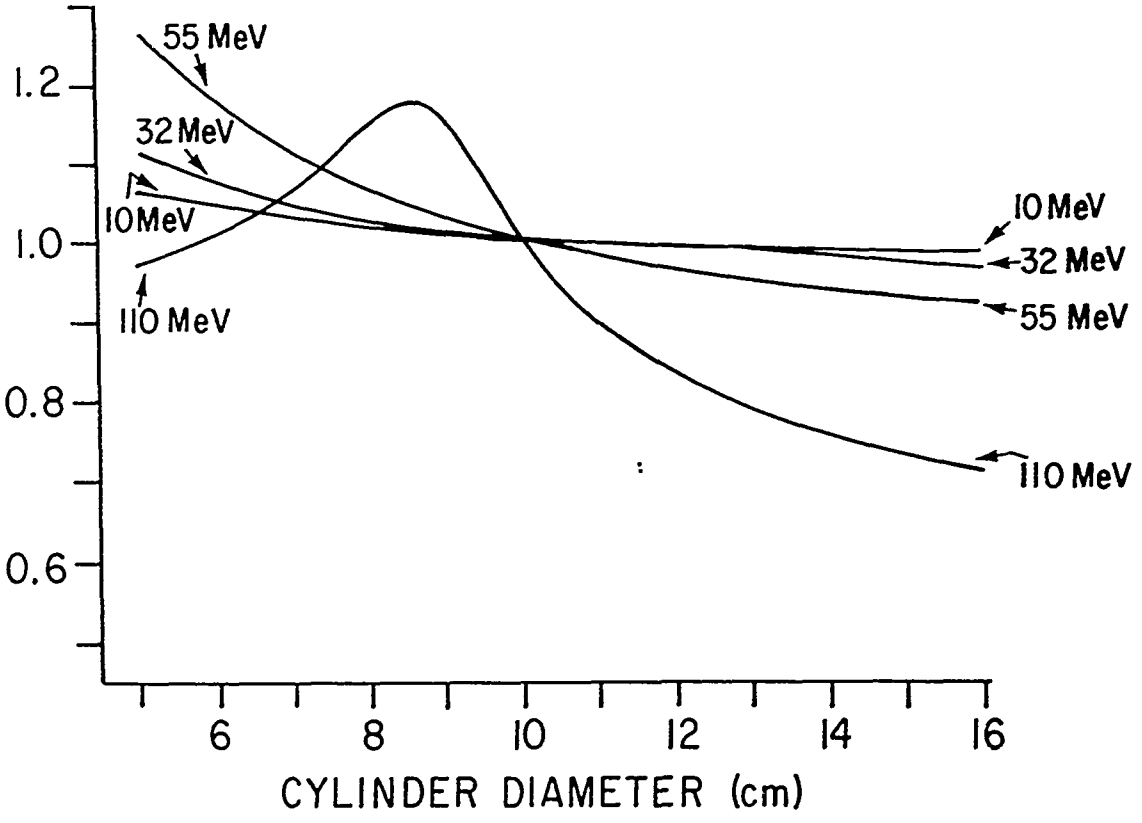

Figure 2. Relative surface dose for cylinders from radius 5 cm to 15 cm. All doses are normalized to 1.0 on surface of 10-cm diameter cylinder.

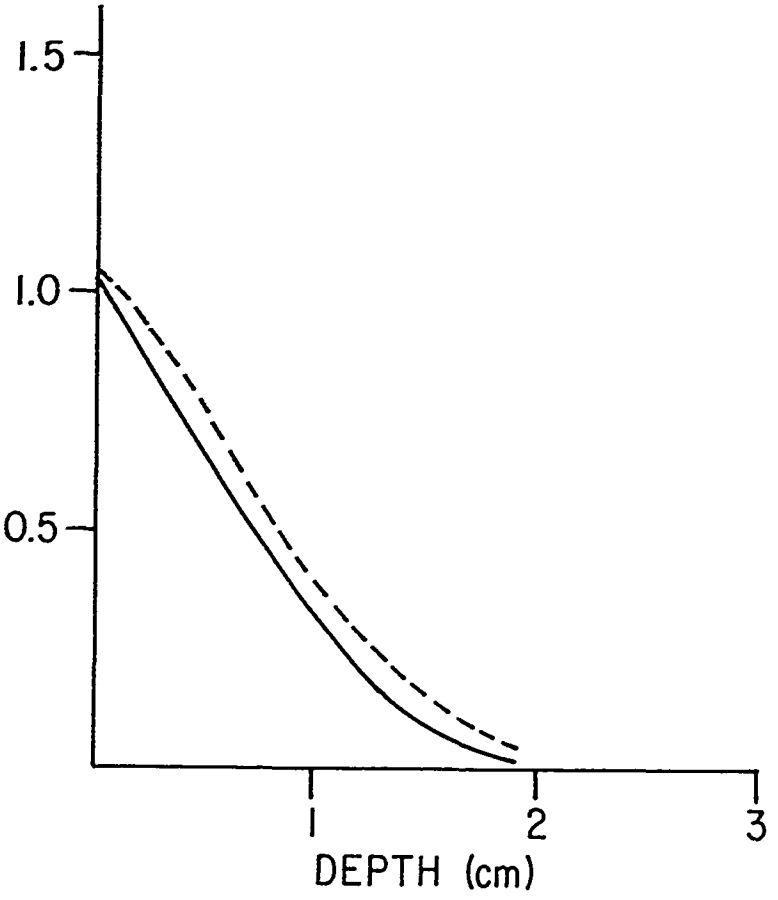

Figure 3A. Relative depth dose to primate eye vs. depth dose to 8-cm diameter cylinder for 10-MeV protons.

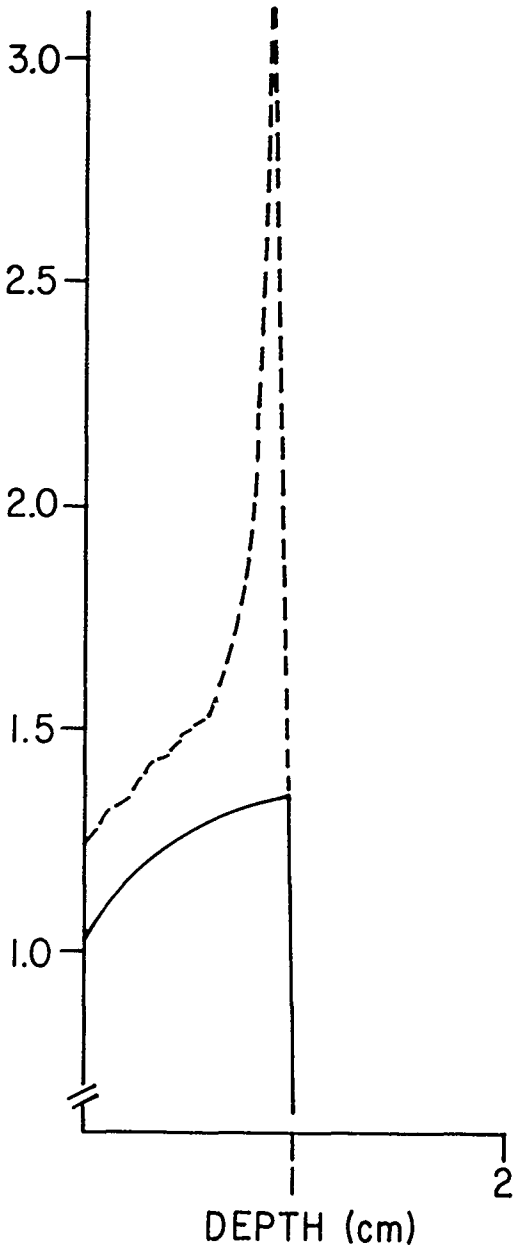

Figure 3B. Relative depth dose to primate eye vs. depth dose to 8-cm diameter cylinder for 32-MeV protons.

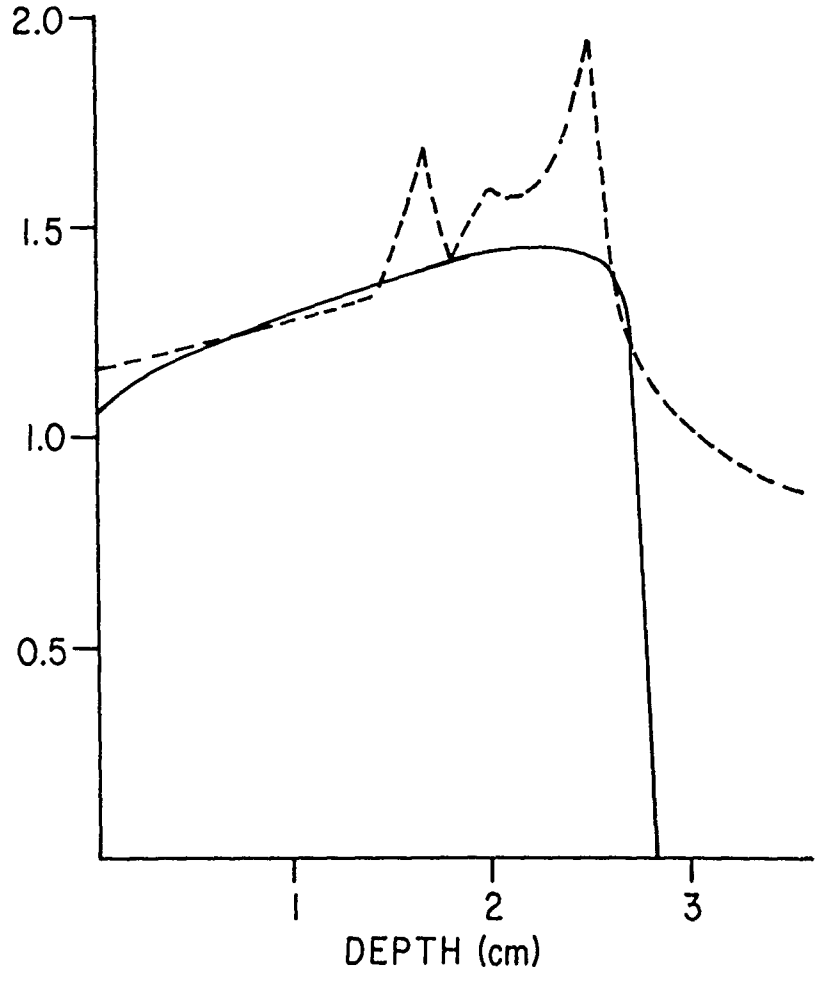

Figure 3C. Relative depth dose to primate eye vs. depth dose to 8-cm diameter cylinder for 55-MeV protons.

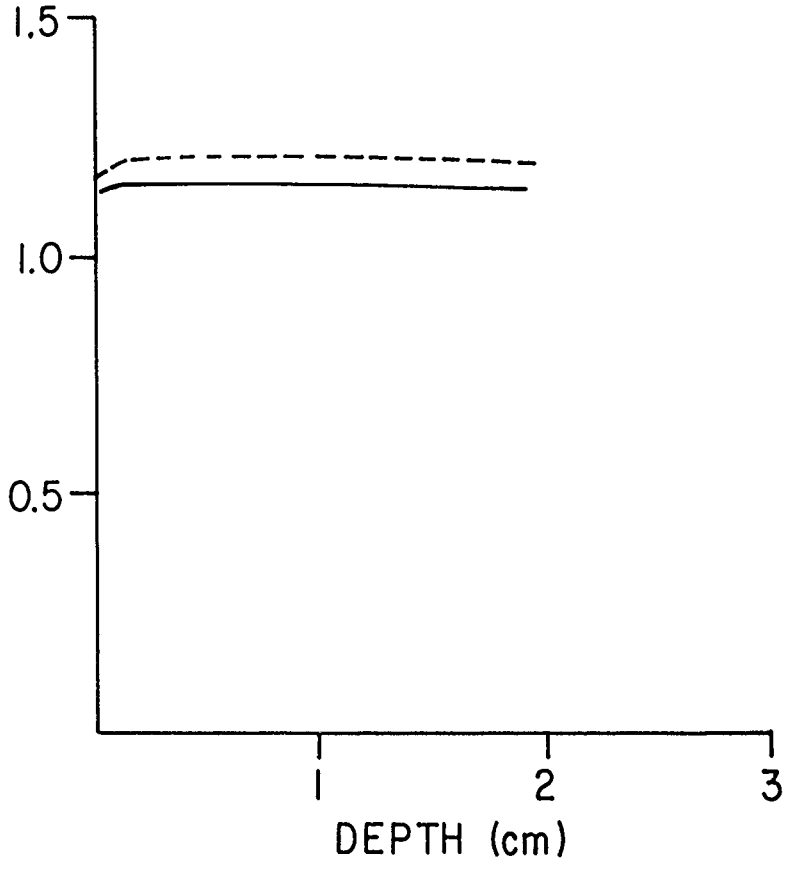

Figure 3D. Relative depth dose to primate eye vs. depth dose to 8-cm diameter cylinder for 110-MeV protons.

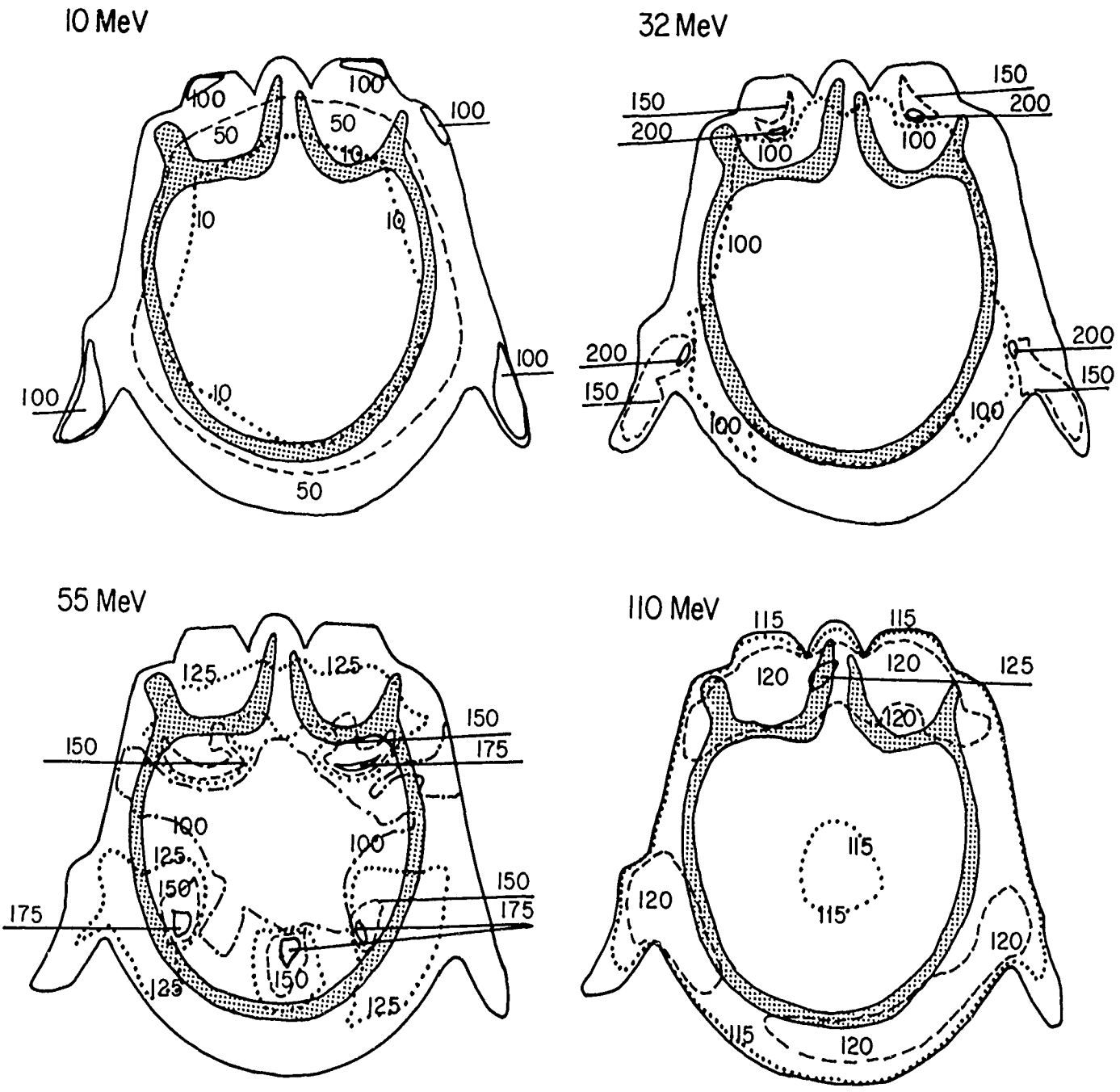

Figure 4. Isodose distributions in plane through eyes. Upper left: For 10-MeV protons, the highest dose level through the eyes is on the front surface of the eyes. Upper right: For 32-MeV protons, the highest dose level through the eyes is at a depth of 0.85 cm, corresponding to the depth of focus of the Bragg peak during the arc. Lower left: For 55-MeV protons, the greatest dose within this plane occurs in the brain behind the eyes. Lower right: For 110-MeV protons, the dose distribution is relatively uniform across the entire plane.

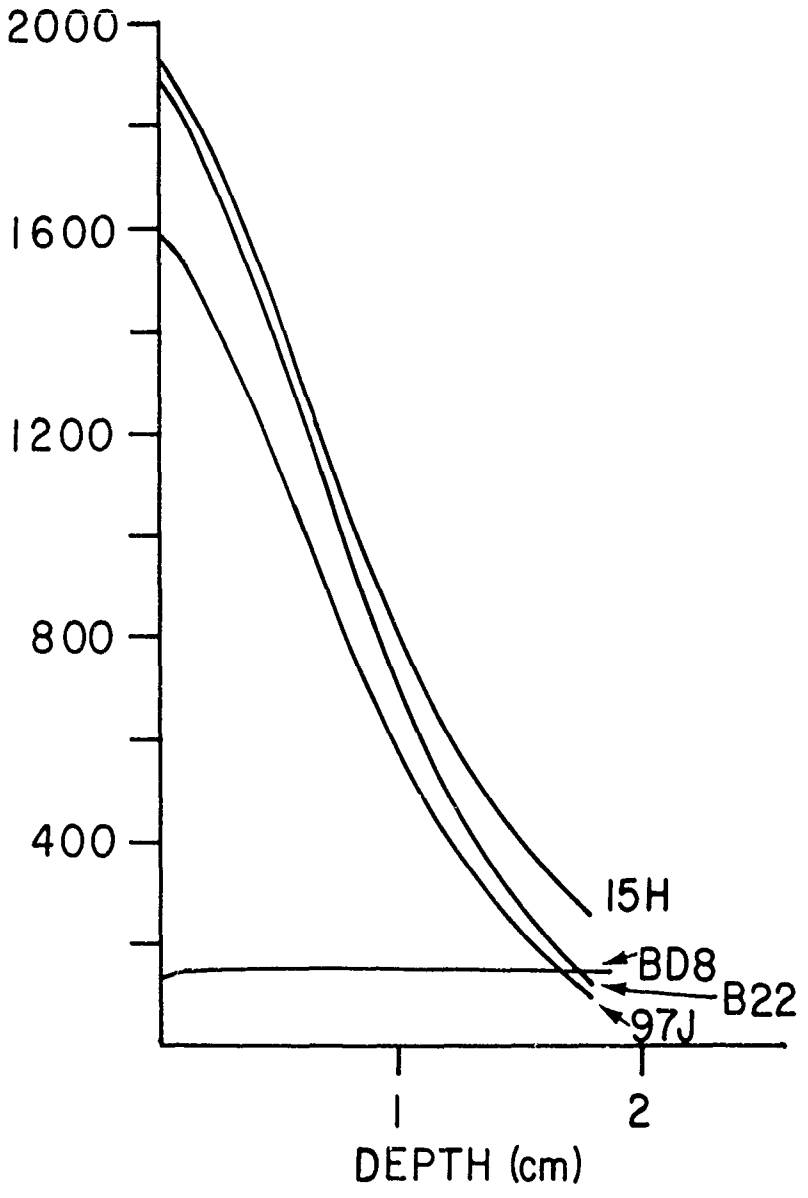

Figure 5. Depth doses through the eye for four irradiation schemes using 10-MeV and 110-MeV protons. Codes attached to each curve represent the primate receiving this irradiation.

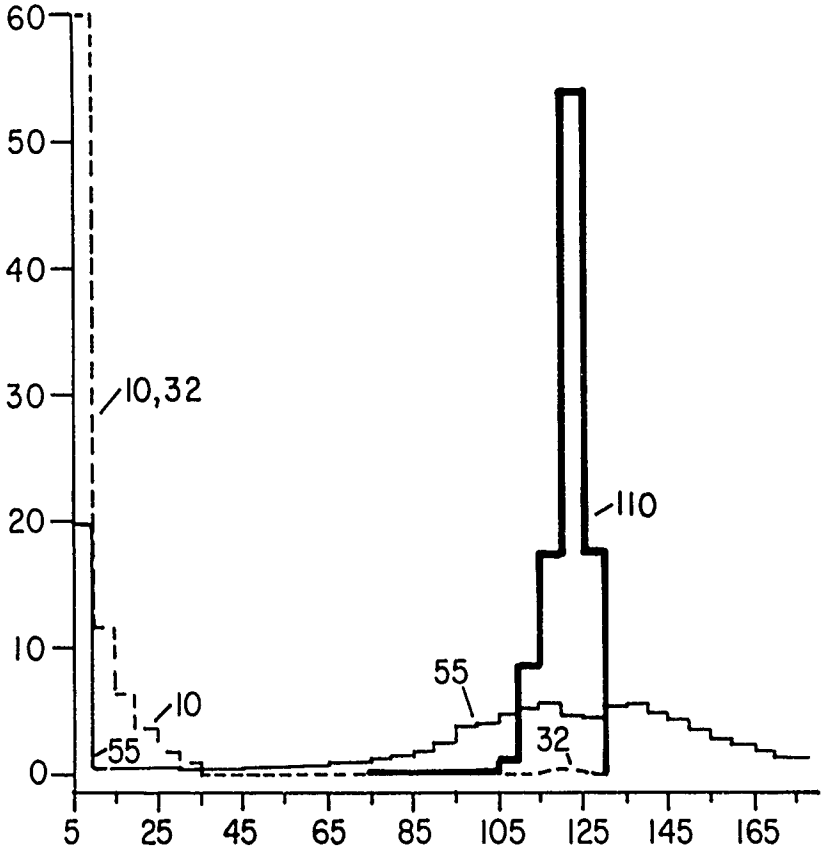

Figure 6. Comparative dose volume histograms for 10-MeV, 32-MeV, 55-MeV and 110-MeV irradiation. Relative doses were normalized to 100% on the surface of a 10-cm diameter cylinder for each energy. Data are plotted as percent of brain receiving relative dose. No significant dose to the brain is received from 10-MeV or 32-MeV irradiation. Over 50% of the brain receives a dose from 100% to 150% of reference surface dose from 55-MeV protons; 96% of the brain volume receives a dose from 105% to 125% of the reference surface dose from 110-MeV protons.

Table 1. PROTON ARC CALCULATED DOSE TO PRIMATE EYE FOR 110-MEV + 10-MEV PROTONS

Depth (cm)	Primate Identifier 15H. BW8.	BR2. BQ0.	BD8. BE8.	68M. 49H.	BF8. 97J.	H34. 69H.	41J. BM8.	BP2. AW6.	BF6. 93H.	AW0. 63H.	BV6. 57H.	BE2. AY4.
						Dose (Centigray)						
0.0	1895	1880	140	1579	1567	117	1264	1254	94	948	632	316
0.1	1836	1814	143	1530	1512	119	1224	1209	95	918	612	306
0.2	1719	1687	144	1433	1406	120	1146	1125	96	860	573	287
0.3	1625	1585	145	1354	1321	121	1083	1057	97	812	542	271
0.4	1501	1452	146	1251	1210	121	1001	968	97	751	500	250
0.5	1396	1340	146	1163	1116	122	931	893	97	698	465	233
0.6	1269	1203	146	1057	1103	121	846	802	97	634	423	211
0.7	1128	1053	146	940	878	121	752	702	97	564	376	188
0.8	1107	923	145	839	769	121	671	615	97	504	336	168
0.9	875	782	145	729	652	121	583	521	97	438	292	146
1.0	784	685	145	654	571	121	523	457	97	392	261	131
1.1	683	578	145	570	481	120	456	385	96	342	228	114
1.2	607	496	144	506	413	120	405	331	96	304	202	101
1.3	526	409	144	438	341	120	351	273	96	263	175	88
1.4	449	327	144	374	273	120	300	218	96	225	150	75
1.5	401	276	143	334	230	120	267	184	96	201	134	67
1.6	341	212	143	284	176	119	227	141	96	170	114	57
1.7	296	164	143	247	136	119	197	109	95	148	99	49
1.8	252	116	143	210	97	119	168	77	96	126	84	42

* U. S. GOVERNMENT PRINTING OFFICE: 1991--561-052/40014